PHYSICAL AND CHEMICAL WEATHERING OF ILLITE IN THE PRESENCE OF OXALATE

By
JENNIFER MICHELLE LATIMER

A thesis submitted in partial fulfillment of
the requirements for the degree of
MASTER OF SCIENCE IN SOIL SCIENCE

WASHINGTON STATE UNIVERSITY
Department of Crop and Soil Sciences

MAY 2010

To the Faculty of Washington State University:

The members of the Committee appointed to examine the dissertation/thesis of Jennifer Michelle Latimer find it satisfactory and recommend that it be accepted.

_____

James B. Harsh, Ph.D., Chair

_____

Markus Flury, Ph.D.

_____

C. Kent Keller , Ph.D.

ACKNOWLEDGMENT

I would like to acknowledge the help of my committee and in particular my advisor, James Harsh. I would also like to acknowledge the assistance of Jeff Boyle, Anita Falen and Louis Scudiero for all of their technical expertise and advice.

PHYSICAL AND CHEMICAL WEATHERING OF ILLITE IN THE PRESENCE OF OXALATE

Abstract

by Jennifer Michelle Latimer, MS
Washington State University
May 2010

Chair: James B. Harsh

Clay minerals in the rhizosphere are subject exposed to organic exudates, such as the oxalate anion, which are metabolites of both plant roots and microorganisms. Silver Hill illite particles (diameter 0.1 to 1μm) were treated with 0.01 and 0.1 M Li-oxalate at pH 8 and 60° C. Lithium chloride treatments as well as untreated illite were used as controls. Chemical analysis of the supernatant did not show selective weathering of aluminum from the illite and did not show a difference between chloride-treated and oxalate-treated samples. X-ray diffraction (XRD) analysis patterns of all samples were analyzed with MudMaster, a software that uses the Bertaut-Warren-Averbach method to determine crystalline strain and sizes of mineral particles. The fundamental illite particle thickness decreased, indicating fewer numbers of 2:1 layers per particle. Increased strain after reaction with oxalate indicated that weathering was not uniform throughout the particle. The SEM and AFM micrographs showed little visual variation among treatments, but subsequent AFM image analysis with GIS showed higher surface area, volume, thickness, and diameter for the untreated particles compared to both LiCl and Li-oxalate (LiOx) treated illite. The AFM analysis also showed a reduction in the average number of layers per particle for both LiCl and LiOx treated samples compared to the untreated illite. Lithium oxalate appears to aid in the separation of illite layers, most likely due to a reduction of charge due to the loss of tetrahedral aluminum. It is not clear if the reduction in particle thickness resulted from the expansion of illite layers or better dispersion of the illite fundamental particles.

Table of Contents

Page

List of Figures

List of Tables

CHAPTER I: INTRODUCTION

1. Previous Work

Clay minerals are fundamental components of soil systems. The types and amounts of clay minerals can affect chemical, physical and biological properties and have a large impact on the type of management strategies that will enhance soil quality and sustainability.

One of the most important clay minerals in temperate environments is illite. It has the basic structure of muscovite mica, a 2:1 layered silicate with a potassium dominated interlayer. Illite has less aluminum in tetrahedral sites compared to other micas with consequent depletion of potassium. Frayed edge sites (FES) where some exchange of potassium and other cations can occur, are characteristic of illite.

The amount of potassium weathered from mica is enhanced by the rhizosphere environment (Hinsinger et al., 1992). Often agricultural producers ignore this natural input of potassium, instead choosing to add the entire K requirement for plants as fertilizer (Barre et al., 2007).

Illite exchange reactions become important in contaminated sites such as the Hanford Site in Washington State (McKinley et al., 2001), where 2:1 mica minerals have the capacity to take up potentially hazardous elements. At the Hanford site, nuclear weapons production during the Manhattan Project produced radioactive wastes; such as Cs-137. Due to the proximity of Hanford to the Columbia River and groundwater aquifers, it is important to human health in the area to understand Cs movement within the system.

Several authors suggest that once cesium-137 is released into the soil system, it is taken up preferentially by micas onto frayed edge sites of micaceous minerals where significant amounts of potassium have been depleted due to weathering (McKinley et al., 2001; Maes et al.,

2008). According to this hypothesis, the frayed edge of the illite collapses over the cesium, preventing its immediate desorption (de Koning and Comans, 2004). Jamsangtong et al., (2004) studied cesium-137 adsorption and desorption in the acidic soils of Thailand. They found that over 98% of cesium added to these soils was sorbed, regardless of input chemicals, while less than 1% of the cesium sorbed was eventually desorbed, indicating some kind of barrier to desorption such as the one suggested by de Koning and Comans (2004).

Understanding Cs desorption from the interlayer of micaceous minerals is fundamental in understanding the potential transport of cesium to water bodies. It is also important to understand Cs desorption in order to make more informed management decisions. Recent studies have shown that several plant species have the potential to bioaccumulate Cs, providing a more permanent management strategy using phytoremediation (Singh et al., 1994, Bystrzejewska-Piotrowska and Bazala., 2008, Kamel et al., 2007). Illite weathering needs to be understood in order to both understand Cs-137 contamination as well as K inputs into the environment.

2. Mechanism of potassium depletion

Potassium depletion from the inner layer of illite provides a natural source of K to crops. Studies have suggested that the depletion of K in the soil solution from plant uptake drives the release of K from illite. The result of this is the expansion of 2:1 layers as K is replaced by Ca, Mg and other hydrated cations. Gommers et al. (2005) varied the amount of potassium in a soil system with a high percentage of cesium-contaminated phlogopite in which willows had been planted. The lower the amount of K in the system, the more K was released from phlogopite due

to mass action, causing higher uptake by willow roots. X-ray diffraction analysis showed that this led to some transformation of phlogopite to vermiculite. These authors suggested that the weathering of phlogopite did not create more frayed edge sites, because Cs was not immobilized by the illite.

Hinsinger et al. (2005) also found that mica weathering was initiated through root uptake of potassium. Phlogopite was brought into contact with ryegrass roots for four days and the uptake of both potassium and magnesium were determined. Potassium uptake increased with time whereas magnesium uptake showed no difference from the control (no mica). Expansion of layers of phlogopite (associated with vermiculitization) was seen along the edges near ryegrass roots. This shows that the ryegrass rhizosphere accelerated expansion of layers, possibly due to organic exudates or K depletion driving phlogopite weathering.

3. Illite weathering by organic exudates

Organic root exudates are products of metabolism within the plant (Dakora and Phillips, 2002). There has been research suggesting that plants use exudates to manipulate the soil environment to provide nutrients in low fertility soils. Some researchers have also shown that plants will change the pH of their environment using exudates (Dakora and Phillips, 2002). These exudates are often a complex mix of acids, proteins, and other molecules (Rovira, 1969). Strom et al. (2004) tested nutrient extraction capabilities of three different organic acids in a low fertility environment (calcareous soil). They determined that high concentrations of organic exudates were needed to extract cations (the exception was phosphorous) at non-acidic pHs.

This type of weathering changes a mineral's properties and general chemistry. Research done in the area of mica weathering has suggested that organic acids accelerate weathering at

edge sites. Boyle and Voight (1967) observed morphology of weathered biotite in high acid conditions. There was a marked expansion of edge sites. Boyle and Voight (1967) attributed this to the loss of iron in the octahedral sheet and then subsequent dissolution of edges. Boyle and Voight (1974) later reacted four types of common organic acids (oxalic, malonic, malic, propinoic, and lactic*)* at varying times with biotite to determine what types of ions were primarily lost from the clay. Most of the acids removed a larger proportion of aluminum than potassium.

There has been evidence to support that aluminum is selectively removed from the tetrahedral sheet of micas by organic exudates. Paris et al. (1995) ran experiments to determine the capacity for ectomycorhizae to gain potassium and calcium from soils by weathering micas using organic exudates such as oxalate. They placed the hyphal mats on top of a substrate of phlogopite, and saw an increase of oxalate concentration with higher deficiencies of potassium and calcium. The aluminum concentration increased in the agar below the mica, suggesting that the oxalate weathered aluminum from the phlogopite, aiding in the transformation of micas. If aluminum were removed preferentially from tetrahedral sites, the layer charge of mica would decrease, releasing K to maintain charge balance.

Wendling et al. (2004, 2005a) studied cesium-137 sorption and desorption in soils from illite in the presence of oxalate, citrate and mixtures of root exudates at pH 8. It was found that cesium-137 selectivity decreased in the presence of oxalate, while desorption increased. This may be due to the exposure of non-selective sites on the surface of illite. This could result from expansion of illite layers as Al is complexed by oxalate and other compounds. Cesium release increased with the Al-complexing power of the exudate mixture.

Bosbach et al. (2000) used atomic force microscopy to image hectorite particles in acidic conditions. They identified and quantified the reactive surface of the hectorite and found that the edge sites of the mineral were the most reactive and the basal planes were practically unreactive. This suggests that complexation with aluminum occurs at the edge sites of the mineral, changing the morphology so that the particle visually appears to be weathering from the edges. Kuwahara (2008) performed a similar experiment, using in-situ atomic force microscopy and a air/fluid heating system in order determine the mechanism for muscovite dissolution in alkaline conditions. Once again, the edge sites of the mineral dissolved faster than the basal planes. This supports the results seen by Bosbach et al. (2000).

4. Unknowns in the weathering reaction

The leading hypothesis for the mechanism for illite weathering by organic exudates suggests that the exudates complex with tetrahedral aluminum in the clay, decreasing the amount of (negative) layer charge of the mineral that arises from Al for Si substitution (Shata et al., 2003). Removal of tetrahedral aluminum from only exposed edges would result in expansion of the 2:1 layers from the edge inward. The frayed edge site (FES) concentration could increase as a result, escalating the sequestration of weakly hydrated cations such as K and Cs. If the Al dissolution extends far enough, or occurs along the basal plane, expansion may occur across the entire layer exposing non-selective basal sites, decreasing Cs and K sequestration. It is therefore important to understand the mechanism by which illite is weathered in the rhizosphere in order to determine the long-term consequences of the reaction.

5. Objectives

In this study we aim to determine the mechanism of illite weathering by oxalate under alkaline conditions by observing changes in illite morphology and structure as well as chemical dissolution of Si, Al, and K.

6. Hypothesis

A decrease in selectivity for interlayer cesium and potassium in illite occurs when reacted with oxalate. Our working hypothesis is that decreasing selectivity results from the exposure of non-selective sites on the surface of the mineral. There are two specific hypotheses to account for this phenomenon. First, frayed edge sites are altered by oxalate, so that they no longer collapse over cations such as cesium and potassium. The selective removal of tetrahedral aluminum and the resultant loss of negative charge may cause this. The second hypothesis is that non-selective basal sites are exposed due to layer expansion and subsequent reduction of the number of layers per particle. Testing of these hypotheses requires chemical analyses of ions lost from dissolution, examination of particle morphology and dimensions using atomic force microscopy; as well as determination of particle size and strain using x-ray diffraction.

7. Approach

In order to test the hypothesis, we performed batch experiments using aqueous concentrations of oxalate near the upper limit of rhizosphere concentrations. Oxalate concentrations are most likely significantly higher in the rhizosphere than in bulk soil, and have been found as high as 0.08 *M* (Strom et al., 2004). Also, in order to reduce reaction time, we carried out the weathering reaction at elevated temperature.

Both hypotheses depend on the fact that aluminum is more rapidly removed from illite than silica. The amount of negative layer charge will decrease if aluminum is selectively removed from the tetrahedral sheet. Non-stoichiometric loss of Al relative to Si is a strong indicator of such selective removal. The location of origin of the dissolved aluminum cannot be determined from this method, however.

A change in morphology of the clay particles should be evident for either hypothesis. If the edge site hypothesis is correct, the potassium on the edges will be replaced with the smaller lithium and there may be visible disruption. If weathering extends far enough inward, particle thickness should vary across the particle and strain should increase. Extensive particle dissolution will reduce average particle diameters. If expansion occurs across whole layers, lithium will replace much of the interlayer potassium and the average number of illite layers per particle will decrease. Microscopic imaging techniques, such as scanning electron microscopy (SEM) and atomic force microscopy (AFM), are utilized to provide visual evidence of the opening of FES and determine individual particle thickness, diameter, surface area and volume. For the AFM images, image analysis of a large set of individual particles is used to determine the average properties of the sample. We use analysis of x-ray diffractograms to determine overall average particle properties, including size, thickness surface area and strain. In order to determine surface area and volume of individual particles and to provide 3D visual representation of particle topography we integrate AFM images into ArcGIS software.

8. **Summary**

The weathering reactions of illite are important for several reasons. The first is agricultural, in that illite weathering affects the concentration of an important plant nutrients, potassium and ammonium. The second is geochemical, since illite can temporarily sorb radioactive elements such as cesium-137, which could restrict its availability to plants and humans. Illite weathering in the rhizosphere is enhanced in the chemical environment of the rhizosphere. This environment includes plant root and microbial exudates that complex strongly with aluminum and can accelerate aluminosilicate dissolution. Through chemical, diffraction, and image analysis, we wish to examine the extent of oxalate-accelerated dissolution of illite and the resulting changes in structure and morphology of illite.

CHAPTER II: PHYSICAL AND CHEMICAL WEATHERING OF ILLITE IN THE PRESENCE OF OXALATE

9. Abstract

Clay minerals in the rhizosphere are subject to the presence of organic exudates, such as the oxalate anion, which are metabolites of both plant roots and microorganisms. Silver Hill illite particles (diameter 0.1 to 1μm) were treated with 0.01 and 0.1 M Li-oxalate at pH 8 and 60° C. Lithium chloride treatments as well as untreated illite were used as controls. Chemical analysis of the supernatant did not show selective weathering of aluminum from the illite and did not show a difference between chloride-treated and oxalate-treated samples. X-ray diffraction (XRD) analysis patterns of all samples were analyzed with MudMaster, a software that uses the Bertaut-Warren-Averbach method to determine crystalline strain and sizes of mineral particles. The fundamental illite particle thickness decreased, indicating fewer numbers of 2:1 layers per particle. Increased strain after reaction with oxalate indicated that weathering was not uniform throughout the particle. The SEM and AFM micrographs showed little visual variation between treatments, but subsequent AFM image analysis with GIS showed higher surface area, volume, thickness, and diameter for the untreated particles compared to both LiCl and Li-oxalate (LiOx) treated illite. The AFM analysis also showed a reduction in the average number of layers per particle for both LiCl and LiOx treated samples compared to the untreated illite. Lithium oxalate appears to aid in the separation of illite layers, most likely due to a reduction of charge due to the loss of tetrahedral aluminum. It is not clear if the reduction in particle thickness resulted from the expansion of illite layers or better dispersion of the illite fundamental particles.

10. **Background**

Clay minerals are an essential part of a soil system. They regulate soil chemistry, change physical properties, and support life within a soil. Illite is a 2:1 clay mineral with a high layer charge, generally derived from mica. Illite has less charge than muscovite due to a lower Al to Si ratio in the tetrahedral sheets. In temperate climates, illite often occurs as an intergrade mineral, interstratified with smectite. According to one model, illite/smectite (I/S) fundamental particles possess illite layers on the inside and smectite layers on the exposed or hydrated surfaces (Nadeau, 1999; Eberl et al., 1998; Srodon et al., 1992). As the number of smectite layers increase, the fundamental particle thickness decreases. While most studies have focused on the transformation from smectite to illite, the weathering of illite may in fact be the reverse of this reaction with illite losing tetrahedral Al and negative layer charge (Sucha et al., 2001; Wendling et al., 2005a).

Wendling et al. (2004, 2005b) found that in the presence of oxalate and citrate, and mixtures of rhizosphere microbial exudates, illite surface chemistry changed with respect to cesium exchange reactions. Cesium was more easily desorbed from illite and the selectivity of cesium with respect to sodium and calcium decreased. Cesium desorption was correlated with the formation of aluminium-exudate complexes found in the rhizosphere (Wendling et al., 2005b). A comparison of illite extracted from bulk and rhizosphere associated soils at the Idaho National Laboratory showed the same patter for rhizosphere illite (Wendling et al.,2005a). In a rhizosphere environment in which organic anion concentrations can be high (>50 mM) (Wendling et al., 2005a) aluminum may be lost from tetrahedral sites at a more rapid rate than silica, reducing charge and changing illite layers to be more “smectite-like”.

High affinity sites for cesium and other weakly hydrated cations are located along the edges of illite where expansion of layers due to hydration allows exchange reactions to occur (deKoning and Comans, 2004). When these "frayed edge sites" (FES) collapse around a weakly hydrated cation, its potential to exchange with soil solution cations becomes very low (deKoning and Comans, 2004; Liu et al., 2003). The loss of cesium selectivity when illite is exposed to organic acid anions, could result from a loss of FES, an increase in low affinity sites, or both. If aluminum is lost at the edges of the mineral, the frayed edge sites could expand and become less selective. If the reaction occurs at basal surfaces or propagates rapidly from the edge, the hydration could occur across the interlayer resulting in an increase of "smectite-like" layers. This would reduce the numbers of layers per fundamental particles and expose more low affinity sites.

The objective of this work was to determine the mechanism for the relative loss of high affinity sites in illite weathered by oxalate anions. We used chemical, structural and microscopic analysis to determine fundamental changes in illite reacted with oxalate solutions.

11. **Materials and Methods**

Clay preparation

Clay was obtained from the Source Clays Repository of the Clay Minerals Society--IMt-1 from Silver Hill, Montana (Cambrian shale) characterized by Hower et al. (1966). The illite was crushed in a ball mill overnight to disaggregate. The resulting powder was washed three times with 0.1 *M* NaCl, once with 1*M* Na acetate and dialyzed against deionized water until the electrical conductivity of the solution was below 5 dS m^{-1} (Sposito and Le Vesque, 1985). The

illite was fractionated by centrifugation to collect the 0.1 to 1 μm size fraction according to Stoke's Law. The density of the clay suspension was determined gravimetrically.

Batch experiments

In order to carry out the batch experiments, 0.5 grams of dried clay equivalent were put into a 50 mL plastic bottle with 25 mL of treatment solution. The treatment solutions consisted of 0.1 *M* Li-oxalate, 0.01 *M* Li-oxalate, 0.1 *M* LiCl (the chloride was used as a control) and 0.01 *M* LiCl in triplicate. A portion of the clay was washed only with deionized water and left at room temperature. The bottles containing the solutions were then placed inside a 60° C oven for 30 days. The bottles were not shaken. The pH was maintained daily at pH 8.0 by adding NaOH. The treated and untreated samples were then washed with 10^{-4} *M* HCl.

Intercalcation with akylmamine

To determine if weathered illite was more susceptible to intercalation by alkylammonium ions, we reacted untreated Silver Hill illite with 25 mL 0.5 *M* octylamine (octan-1-amine) in a 60° C oven for ten days. Preliminary experiments on unreacted illite showed ten days was sufficient to remove a significant amount of interlayer K. For this experiment 25 mL of 0.5 *M* octylamine was reacted with illite for varying amounts of time in a 60° C oven. Illite reacted with 25 mL DI water and 25 mL octylamine without illite acted as controls. Amine-treated samples were run on the XRD, and images were obtained by both scanning electron and atomic force microscopy.

Chemical analysis

We determined Al, Si and K concentrations in the supernatant solutions from the batch experiments after 30 days. Solutions were analyzed using inductively coupled plasma (ICP) emission spectroscopy. Statistical comparisons among treatments were made with one-way analysis of variance using the Minitab software program (Minitab 15). Differences were tested using Tukey's pair-wise comparisons.

XRD and MudMaster analysis

Portions of the reacted clays were dialyzed overnight and washed several times with water. They were then mixed with polyvinylpyrrolidine (PVP) (according to the ratio outlined by Eberl et al. (1998). The PVP-illite was then run on the XRD and the pattern was analyzed using MudMaster (Eberl et al. 1996). The XRD patterns had a step size of $0.02^{o}2\Theta$ and were analyzed from 2 to $50^{o}2\Theta$. Since some of the XRD patterns displayed extremely small 2^{nd} and 5^{th} order reflections, all the patterns were analyzed for volume weighted mean thickness and strain using the 1^{st} (4.4-$9^{o}2\Theta$), 3^{rd} (25-31.5 $^{o}2\Theta$), and 4^{th} (31.5-36.4 $^{o}2\Theta$) order reflections of the illite 001 line. Mineral type was set to PVP illite. The d-spacing value for approx. thickness was set to ten, and all other values were set to values specified for PVP illite by Eberl et al (1996).

SEM analysis

A portion of the treated clays were diluted to 0.5 mg mL^{-1} and then 0.5 mL was placed on a SEM carbon tab and dessicated for 24 hours. Images were taken of the two treatments and the untreated clay. A Hitachi S-570 instrument was used. The working distance was 15 cm and the accelerating voltage was 12 kV. Individual particles and groups of particles were scanned.

AFM analysis

In preparation for AFM imaging, illite was placed in the oven for 30 days in 25 mL of pH 8 0.1 *M* Li-Ox and 0.1 *M* LiCl in a separate batch experiment. The clay was extracted and then washed with 0.001*M* lithium oxalate and diluted to 0.005 mg/L. The solution was sonicated using a Heatsystems Ultrasonic sonicator with a titanium probe for 3 minutes at 18,000 watts and then 20 μL aliquot was pipetted onto mica slides and placed in a 40° C oven overnight. A Digital Instruments Nanoscope III was used in collaboration with Dr. Louis Scudiero. A 100 X 100 μm image was taken in contact mode and split into a 5 by 4 grid. Three areas were selected using a random number generator, and a 20 X 20 μm image was taken of the area, and each particle was subsequently imaged using a 5 X 5 μm scan. Using the built-in AFM software, width and height were measured with the section analysis tool (Figure 1).

Subsequently, each image was transformed into a TIFF file and then imported into Adobe Photoshop where the images were cropped in order to isolate just the imaged area (Figure 2). The ArcGIS 3D surface volume tool was used in order to determine surface area and volume of the particles (Figure 3). The surface volume tool is a 3D analyst tool that looks at an image and assumes that the brightest pixels have the greatest elevation. Utilizing that assumption, it then calculates the 2D area, 3D volume and 3D surface area. In order to accomplish this, the height values (in nanometers) were input into the metadata. The AFM images were also input into GIS and converted into contour maps. Contour maps are similar to topographic maps in that they show variations in height across a surface. As such, they provide a good indication of the visual location of weathering. The surface area, volume, height, width and difference between edge sites and the middle of the particle were analyzed using ANOVA in Minitab and differences were tested using Tukey's pair-wise comparisons.

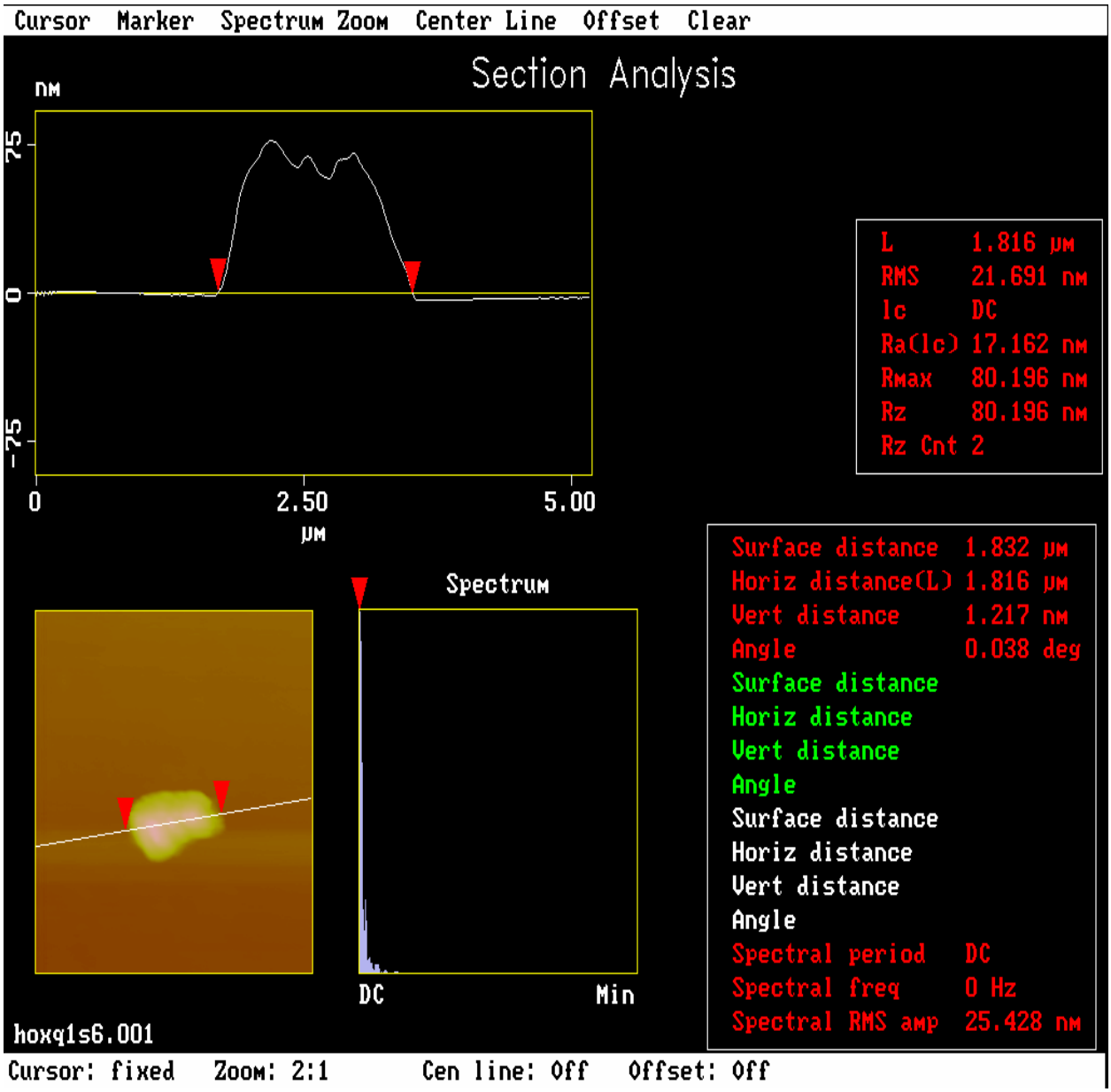

Figure 1: Particle measurements using the section analysis tool in AFM

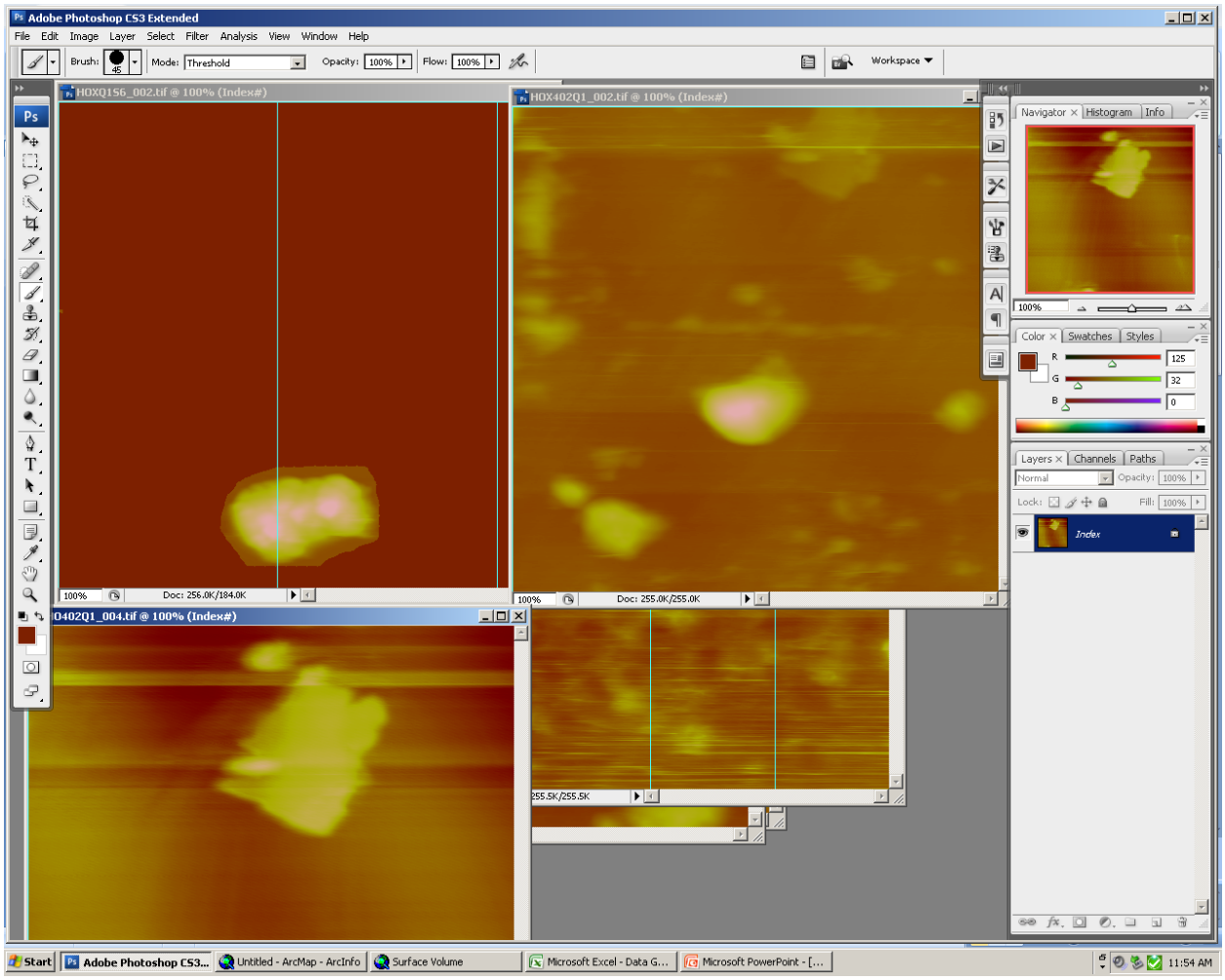

Figure 2: AFM images cropped in Adobe Photoshop

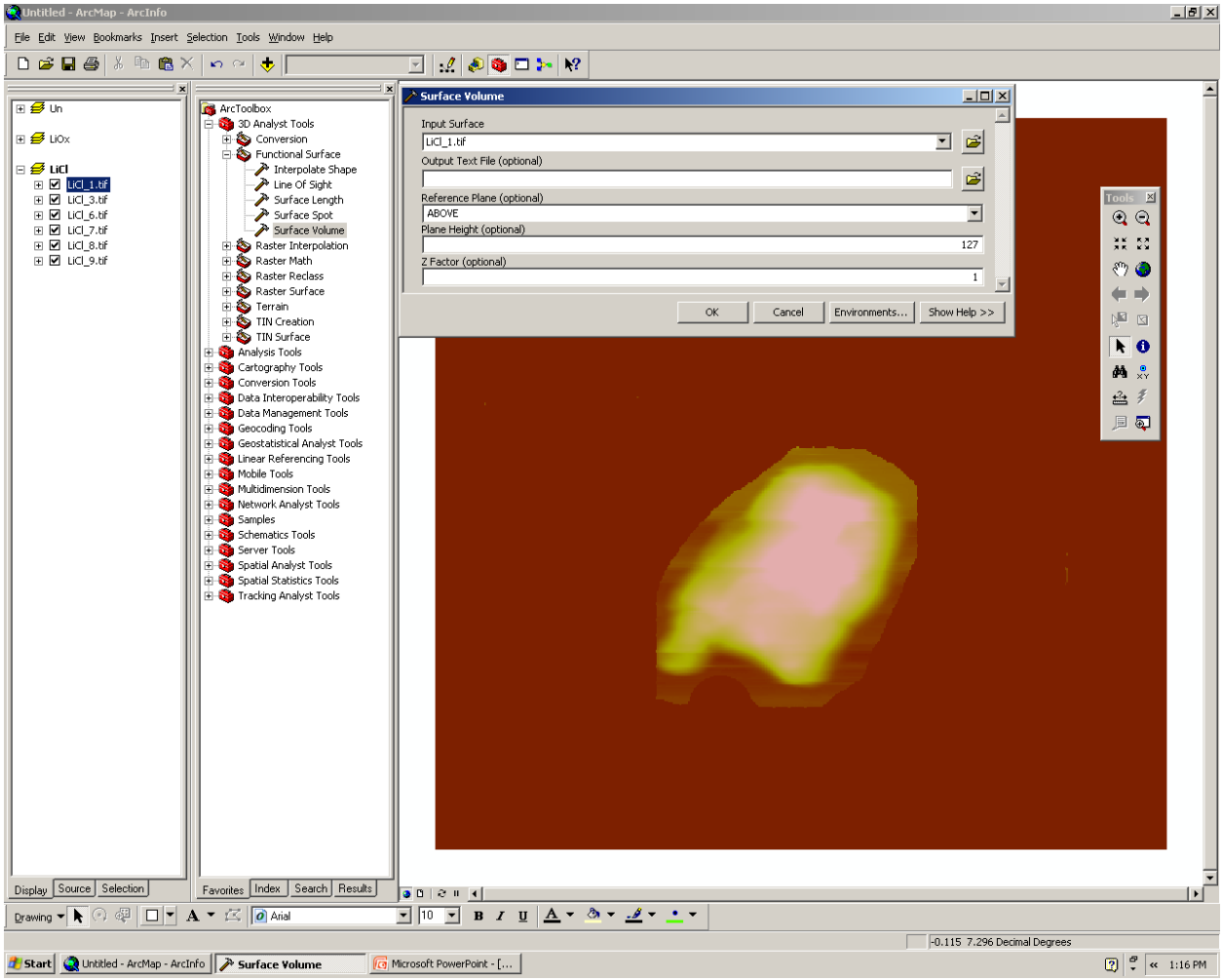

Figure 3: Use of the surface volume tool in GIS to determine volume of the particle

12. **Results**

Amine experiments

To determine if reaction with oxalate weakened the illite structure, in particular its ability to expand, we treated weathered illite with octylamine. The ideal exposure time for amine to be exposed to illite was ten days due to the moderated loss of K from the mineral. Although no statistically significant difference was seen in amount of time of exposure, ten days showed a moderate amount of K loss.

The amine treated LiCl and Li-Ox particles were difficult to image and to create into XRD images. The particles formed aggregates due to the positive charge on the octylamine ions. The aggregates made it difficult to isolate particles for imaging, so they did not provide good data for comparative particle measurements.

Chemical Analysis

The supernatant solutions were analyzed for Al, Si and K to determine the stoichiometry and extent of illite weathering. The 0.01 *M* Li-Ox treated illite released significantly larger amounts of all Al and Si ions compared to the 0.1*M* Li-Ox and 0.1 and 0.01 *M* LiCl. The other treatments did not show a significant difference (Table 1). Al and Si showed high variability, but the same significance pattern was seen in the potassium, which had a low level of variability. The low released ion levels were unexpected for the 0.1 Li-Ox since Al-oxalate complexation should be a fundamental part of illite dissolution.

Table 1: Mean supernatant solution Al, Si, K concentrations (n=3). Values that are not significantly different (p=0.05) are denoted with the same letter.

Treatment	Al mmol/g clay	K mmol/ g clay	Si mmol/g clay	significance
0.1 *M* LiOx	0.03 +/- 0.03	0.02 +/- 0.00	0.05+/- 0.06	a,a,a,
0.01*M* LiOx	0.10 +/- 0.02	0.03 +/- 0.01	0.19 +/- 0.04	b,a,b
0.1*M* LiCl	0.02 +/- 0.01	0.01 +/- 0.00	0.03 +/- 0.03	a,a,a,
0.01*M* LiCl	0.04 +/- 0.02	0.02 +/- 0.00	0.07 +/- 0.05	a,a,a,

To determine the stoichiometry of illite dissolution, we compared the released ion ratios of Al/K, Al/Si and Si/K to the Silver Hill illite solid phase (Hower and Mowatt, 1996). The ratios of Al/K, Al/Si, and Si/K showed non-normal distribution and so could not be analyzed by ANOVA; however, the log(experimental ratio/untreated ratio) values had normal distribution. When the log values were analyzed by ANOVA, there were no statistically significant differences among treatments. All samples showed selective weathering of Si relative to both Al and K (Table 2). Surprisingly, incongruent dissolution of Al was seen in all treatments, but the proportion dissolved was less than its proportion in the illite.

Table 2: Mean ratios of dissolved log concentrations compared to solid state ion concentrations for Al/Si, Al/K, and Si/K (n=3). Values that are not significantly different (p=0.05) are denoted with the same letter.

Treatment	log (Al/Si/solidAl/Si)	log(Al/K/solidAl/K)	log(Si/K/solidSi/K)	significance
0.1*M* LiOx	-0.50 +/- 0.27	0.31+/-0.27	0.80 +/-0.50	a,a,a
0.01*M* LiOx	-0.70 +/- 0.01	0.62 +/- 0.01	1.32 +/-0.00	a,a,a
0.1*M* LiCl	-0.70 +/- 0.07	0.11 +/- 0.33	0.78+/-0.35	a,a,a
0.01*M* LiCl	-0.71 +/-0.03	0.25 +/- 0.35	0.96 +/- 0.32	a,a,a

SEM Analysis:

Scanning electron microscopy provided a means to examine weathering effects on particle morphology at the micrometer scale. There are no apparent differences at this scale, indicating that weathering under the short batch conditions are subtle and must be probed by other means (Figure 4). This is not surprising given that the highest dissolution of illite according to the Si chemical analysis was about 2%. Images were chosen because of their clarity.

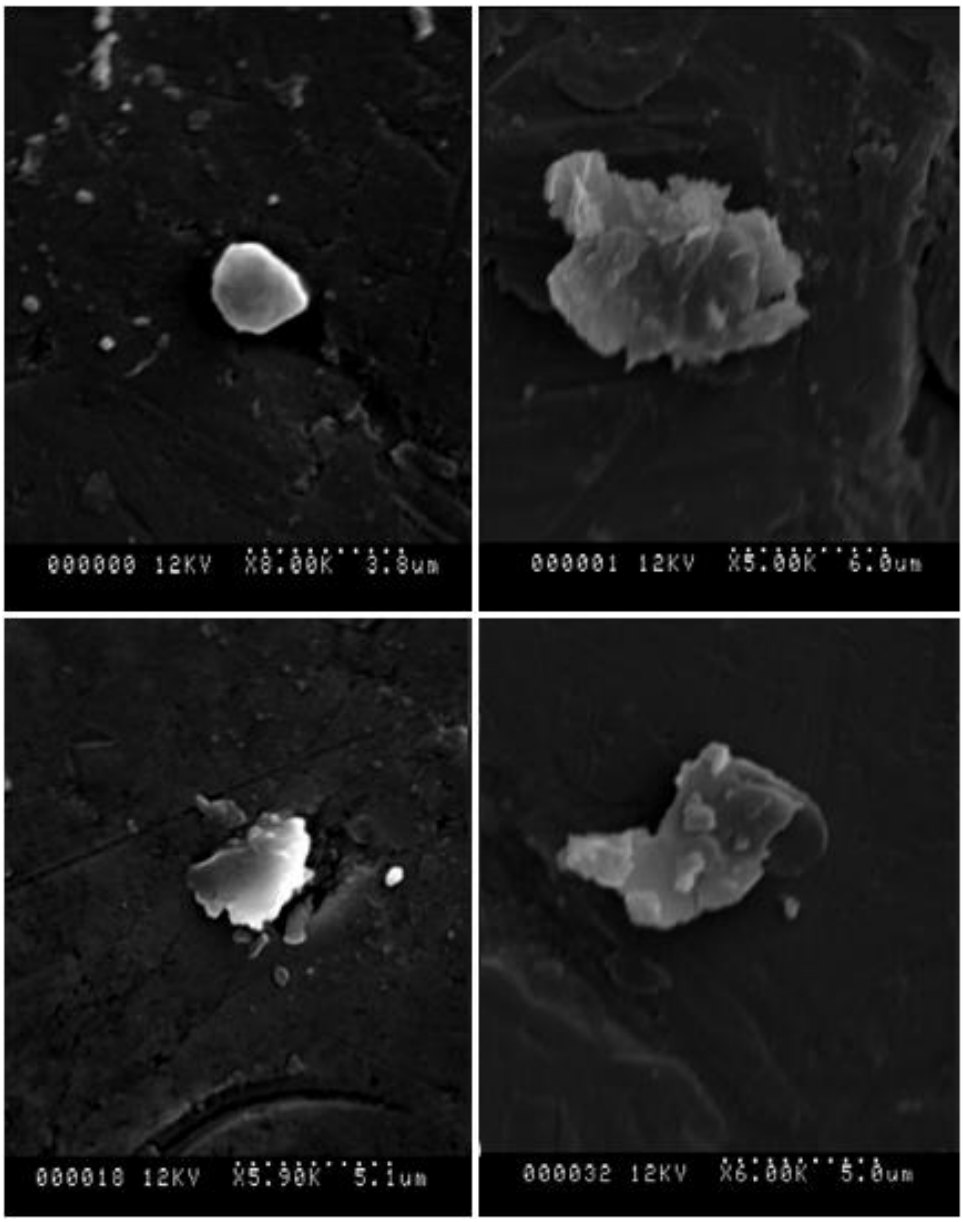

Figure 4: SEM images of particles. Top Left: Untreated Top Right: 0.1*M* LiOx Bottom Right: 0.01*M* LiOx Bottom Left: 0.1*M* LiCl

XRD Analysis

We used x-ray diffraction as a means to understand structural changes in weathered illite. The patterns themselves show little variation (Figure 5), in terms of peak position or intensity, although there are small, unidentified peaks around 22 and 28°2Θ in all of the treated samples.

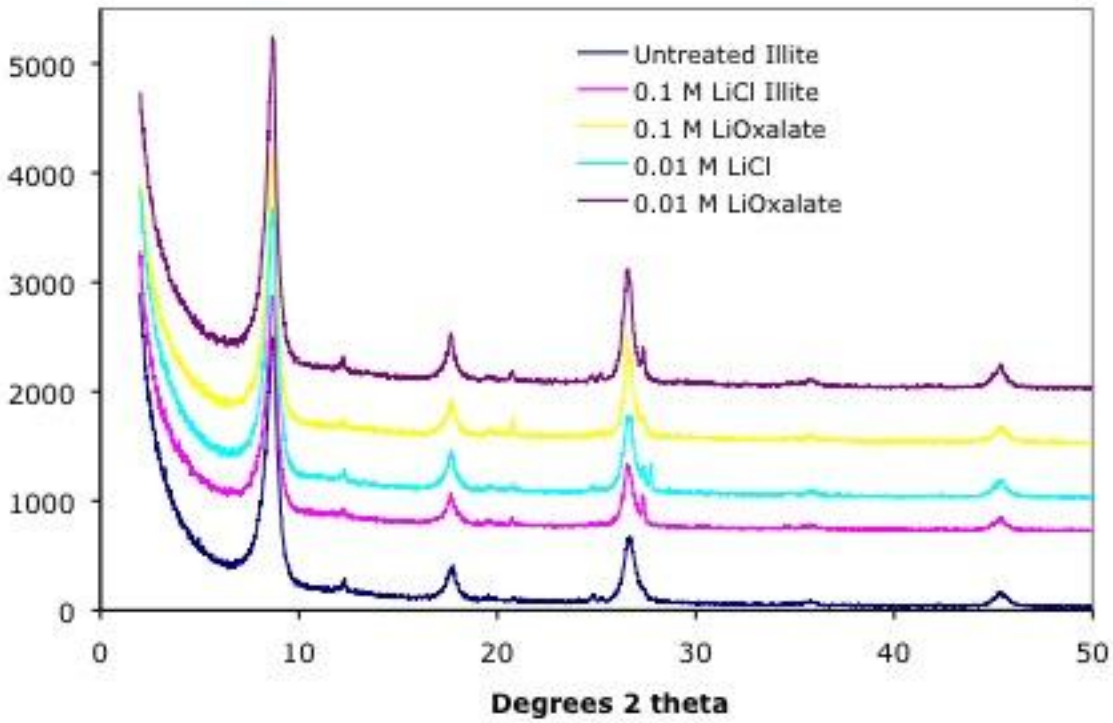

Figure 5: X-ray diffraction patterns of treated samples and unreacted 0.1 – 1.0 μm Silver Hill illite used for MudMaster analysis of particle size parameters and strain. The patterns are shifted vertically for clarity.

MudMaster Analysis

The X-ray diffraction patterns were analyzed with Mudmaster in order to determine changes in illite particle size and strain with treatment. Strain measures small fluctuations in the thickness of the particles. Reduction in thickness indicates fewer numbers of layers per illite particle, whereas strain indicates uneven weathering across the particles leading to areas of more or less layer expansion. The MudMaster results show that particle thicknesses decrease with oxalate treatment, the largest decrease occurring in the 0.01*M* oxalate treatment (Figure 6). Particle thickness slightly decreases with all of the treatments, but is more pronounced in the oxalate treatments.

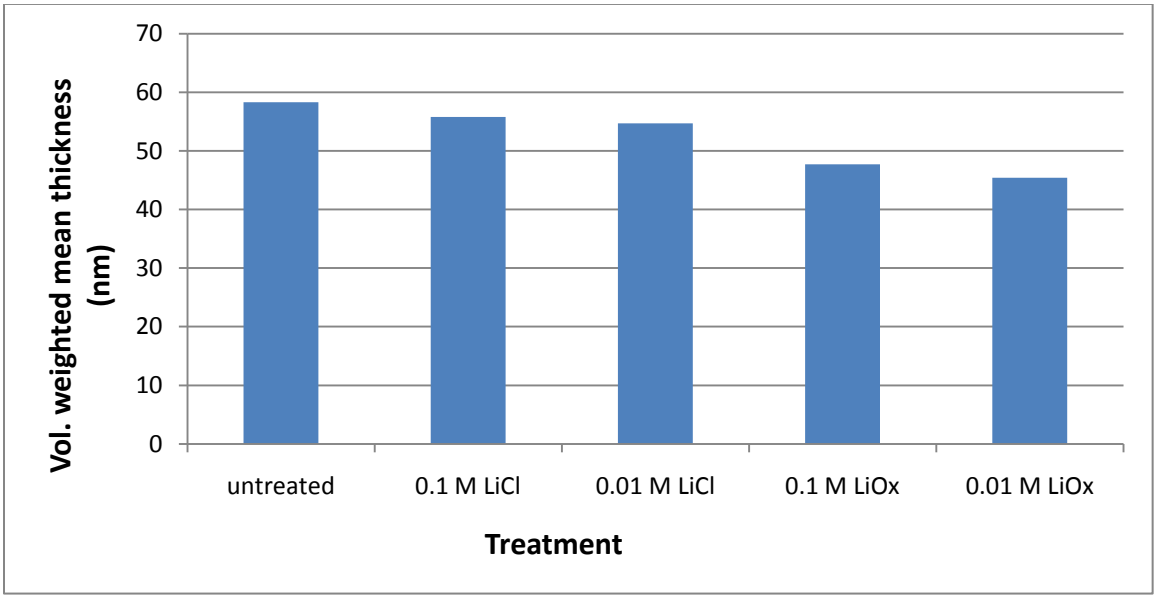

Figure 6: Volume weighted mean thicknesses as calculated by MudMaster for four different treatments

Higher strain was found in the oxalate treatments. Strain indicates small variations in the d-spacing of illite, indicative of nonuniform weathering and expansion across particles. The untreated particles showed slightly higher strain than the Li-Cl treated particles (Figure 7). The 0.01 *M* oxalate treatment resulted in the highest strain, whereas the 0.01 *M* chloride treatment resulted in the smallest.

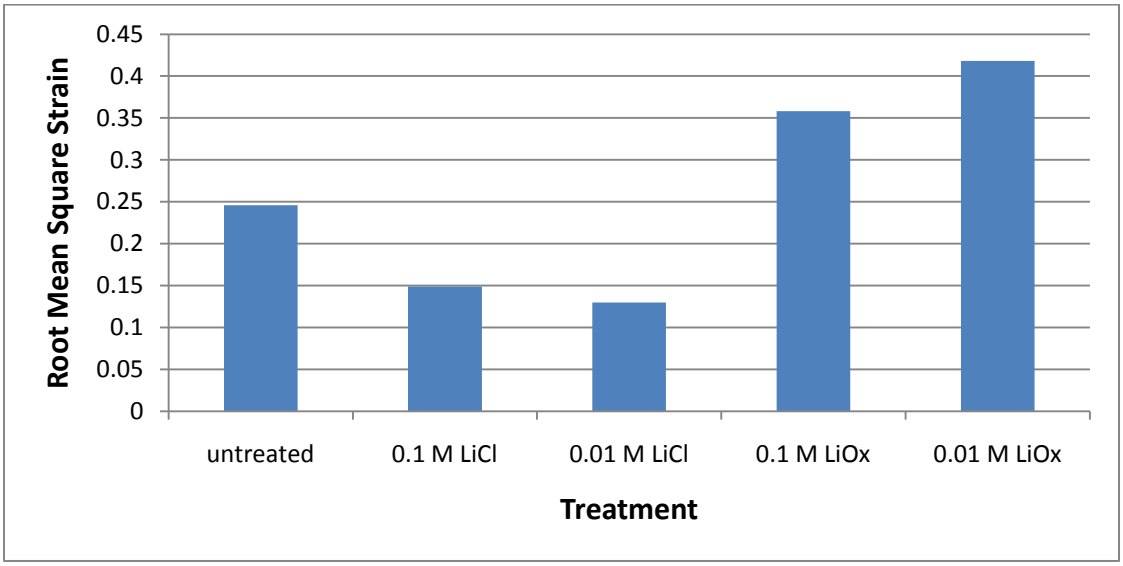

Figure 7: Root mean squared strain as calculated by Mudmaster for four different treatments

AFM Analysis

We used atomic force microscopy (AFM) to probe weathering of individual particles at the nanometer scale. Morphology, size, surface area, and volume of particles in each treament were determined. We only used .1 *M* Li-Ox and Li-Cl due to time and cost considerations. Ten particles were analyzed per treatment.

We used the AFM images to create contour maps to better illustrate particle morphology. The contour maps show large differences between the untreated and Li-treated particles (Figure 8) and slight differences between the Li-Ox and Li-Cl particles. The Li-Ox particle seems to be slightly more weathered on the edges. Around 80 % of the Li-Ox particles showed this rough appearance. These particles were selected for their clarity.

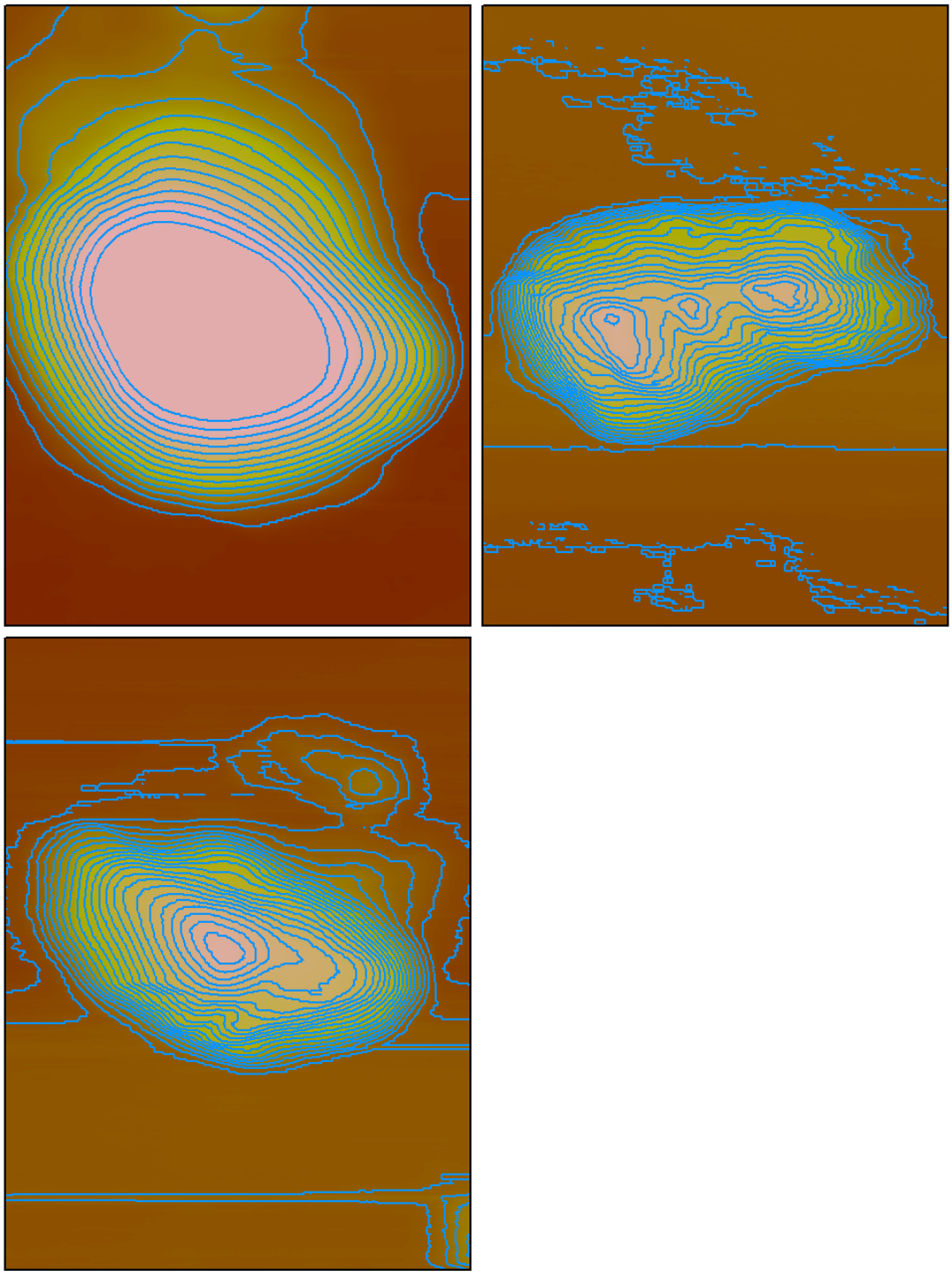

Figure 8: AFM images overlaid with contour intervals. Top Left: Untreated, Top right: 0.1*M* LiOx Bottom Left: 0.1*M* LiCl

We used two types of image analysis to confirm the visual evidence of weathering by Li-oxalate: the AFM to obtain particle dimensions and ArcGIS to determine average particle area and volume. Surface dimensions of the individual particles were obtained using the section analysis tool built in to the AFM. We determined the diameter, right edge, left edge and middle thickness of all of the particles in the defined areas. Differences between edge and middle thicknesses were also determined. The differences between right and left edges were small, so only right edge data was used in the final analysis. The results found by section analysis largely supported the results obtained by MudMaster. The untreated samples showed the largest diameter. The untreated and LiCl samples showed significantly larger edge and middle thicknesses than the oxalate (Table 3). There was a significantly smaller difference in edge and middle thickness in the LiOx sample when compared with the untreated (Table 4).

Table 3: Mean surface dimensions of particles as calculated by the surface analysis tool on the AFM. Values that are not significantly different are denoted with the same letter (p=0.05)

	diameter (μm)	height right edge (nm)	height middle (nm)	difference (middle -right edge) (nm)	Signific-ance
Untre-ated	1.86 +/- 0.40	58.15 +/- 46.10	74.46 +/- 56.00	16.31 +/- 13.66	a,a,a,a
0.1*M* LiOx	1.13+/- 0.43	58.74 +/- 35.70	59.76+/- 39.40	1.02 +/- 5.92	b,a,b,b
0.1 *M* LiCl	0.93 +/- 0.22	68.58 +/- 28.39	76.94 +/- 19.22	8.36 +/- 12.73	b,b,a,ab

Table 4: Mean surface area and volume of AFM imaged particles as calculated by GIS Values that are not significantly different (p=0.05) are denoted with the same letter.

Table 4: Mean surface area and volume of AFM imaged particles as calculated by GIS Values that are not significantly different (p=0.05) are denoted with the same letter.

Treatment	surface area (µm2)	average volume (µm3)	significance
Untreated	48.18 +/- 56.72	23.24 +/- 34.05	a,a
0.1 LiOx	8.828 +/- 6.750	2.015 +/- 1.673	b,b
0.1 LiCl	9.358 +/- 3.9212	2.388 +/- 1.381	b,b

The average surface area and volume of treated particles 0.1 *M* LiCl and LiOx decreased significantly relative to the untreated illite (Table 4). This decrease cannot be due to particle dissolution, because chemical analysis indicated that dissolution did not exceed a few percent of the illite mass. Therefore, the LiCl and LiOx treatments must have separated illite particles into smaller units either by disaggregation or layer expansion. The high variability seen in the samples could be partially due to the variability in the illite particles.

13. Discussion

Chemical Analysis

For the chemical analysis, only the 0.01M LiOx treatment had significantly higher dissolved aluminum, silica and potassium loss from the clay. The reason why the lower concentration of oxalate dissolves more Al than the higher concentration treatment is unclear. A possibility is that aluminum precipitated in the higher concentration solution. This could be the reason for the small non-illite peak seen in the X-ray diffractograms.

Since there is no statistical difference between the log comparisons of the ratios, the hypothesis that oxalate will preferentially release aluminum while being weathered by oxalate

cannot be supported by this data. Both of the solutions selectively dissolve silica and to a certain extent aluminum, but there is no statistical difference between the treatments. The lack of statistically significant results arose from the high variability among replicates. Perhaps more replicates need to be reacted. This was probably caused by secondary reactions, such as Al precipitation that precluded an accurate determination of total Al released from the clay.

XRD and MudMaster

The XRD and MudMaster analysis gave the most compelling results. There is a decrease in thickness when comparing the untreated and oxalate samples. Also, the strain value is the highest in the oxalate sample. Weathering at specific sites such as edges may have caused the higher strain. Edge weathering might explain the thinner particles as well since edge site weathering may cause reduction in the number of illite layers, if it progresses far enough along selected layers.

SEM

While conclusions based on visual images may be somewhat subjective, they can be used to support quantitative data. The "roughed up" appearance of the oxalate particles support the higher strain found by the MudMaster analysis.

AFM

The AFM and subsequent integration into GIS proved to be a valuable tool for analyzing the morphological differences between treatments. Visual examination of particles using TIN and contour intervals showed a roughened edge pattern similar to the one seen with the SEM. Smaller thicknesses in the oxalate particles are consistent with the MudMaster data. The significantly larger difference between middle and edges thicknesses seen in the untreated particles when compared with the oxalate particles were likely due to larger edge thicknesses than middle thicknesses. This may be due to the fact that smaller layers are being removed from the top and bottom of the particle.

14. Conclusions

The chemical data did not show selective weathering of aluminum in the oxalate-treated samples, and in fact did not show much difference between treatments. The hypothesis that tetrahedral aluminum is being selectively removed by oxalate is not supported by the evidence presented here. Yet there is evidence to suggest that the location of illite weathering by oxalate is occurring at both the planar and edge sites. The MudMaster data and AFM data show a significant drop in thickness in the oxalate-treated particles when compared with the untreated particles. This evidence supports the planar hypothesis. The MudMaster results also shows higher strain values for the oxalate treatments, which is supported by SEM and AFM images which show "roughed up" oxalate-treated particles. This evidence supports the edge hypothesis. The significantly smaller difference between middle thicknesses and edge thicknesses is due to most of the oxalate particles having larger edge thicknesses than middle thicknesses. It would be conceivable that the oxalate is weathering both the edge and planar sites simultaneously.

15. Further Work

More research is needed to determine if the mechanism of illite weathering by oxalate is indeed facilitated by the removal of tetrahedral aluminum. More chemical testing will be needed, to confirm if more aluminum is released in the presence of oxalate if illite is being weathered. Both batch and column experiments need to be performed. A column experiment could perhaps eliminate the error associated with performing batch experiments in an oven, and could provide data that would be closer to conditions found in the field. More replicates could also help with some of the repeatability issues with the chemical data. More replicates would also help with the MudMaster data, since it would reinforce the evidence that both edge and planar sites are the location of oxalate weathering. The AFM surveys need to be taken for both 0.01 molar and 0.01 molar concentrations of lithium chloride and lithium oxalate.

BIBLIOGRAPHY

Barre, P., Velde, B. and L. Abbadie. 2005. Dynamic role of "illite-like" clay minerals in temperate soils: facts and hypotheses. *Biogeochemistry*. 82:77-88.

Bosbach, D., Charlet, L., Bickmore,B., and M.F. Hochella. 2000. The dissolution of hectorite: In-situ, real-time observations using atomic force microscopy. *Am. Mineralogist* 85:1209-1216

Boyle, J. R., G. K. Voight, and B. L. Sawhney. 1974. Chemical weathering of biotite by organic acids. *Soil Sci.* 117:42-45.

Boyle, J.R. and G.K. Voight. 1967. Biotite flakes: alteration by chemical and biological treatment. *Science*. 155:193-195

Bystrzejewska-Piotrowska, G, and M.A. Bazala. 2008. A study of mechanisms responsible for incorporation of cesium and radiocesium into fruitbodies of king oyster mushroom (*Pleurotus eryngii*). *Journal of Environ. Radioactivity* 99:1185-1191

Dakora, F.D. and D.A. Phillips. 2002. Root exudates as mediators of mineral acquisition in low-nutrient environments. *Plant and Soil* 24:35-47.

de Koning, A., and R.N.J. Comans. 2004. Reversibility of radiocaesium sorption on illite. *Geochimica* 68:2815-2823

Eberl, D.D.,Nuesch,R.,Sucha,V., and S. Tsipursky. 1998. Measurement of fundamental illite particle thicknesses using PVP-10 intercalation. *Clays and Clay Minerals* 46:89-97

ESRI, 2006. ArcGIS program.Version 9.4 [Computer Software] Redlands,CA; ESRI, Inc

Gommers, A. Thiry, Y. and B. Delvaux. 2005. Rhizospheric mobilization and plant uptake of radiocesium from weathered micas. *J. Environ. Qual*. 34:2167-2173

Hinsinger, P., Jaillard, B. and J.E. Dufey. 1992. Rapid weathering of a trioctahedral mica by the roots of ryegrass. *Soil Sci. Am. J.* 56:977-982

Jamsangtong, J., Parkpian, P., Delaune, R.D., and Jugsujinda A. 2004. Retention of ^{137}cesium in acid sulphate soils of South Central Thailand. *Chemistry and Ecology* 20:241-256

Kamel, H.A., Eskander, S.B., and M.A.S. Aly. 2007. Physiological Response of *Epipremnum Aureum* for Cobalt-60 and Cesium-137 Translocation and Rhizofiltration. *Intl. Journal of Phytoremediation* 9:403-417

Kuwahara, Y. 2008. In situ observations of muscovite dissolution under alkaline conditions at 25–50 °C by AFM with an air/fluid heater system. *Am. Mineralogist.* 93:1028-1033

Liu,C., Zachara,J.M.,Smith,S.C.,McKinley, J.P., and C.C. Ainsworth. 2003. Desorption kinetics of radiocesium from subsurface sediments at Hanford Site, USA. *et Cosmochimica Acta* 67: 2893-2912

Maes, E., Delvaux B., and Y Thiry. 2008. Fixation of radiocaesium in an acid brown forest soil. *Euro. Journal Soil Sci.* 49:133-140.

Mckinley, J.P.,Zeissler, C.J., Zachara, J.M., Serne, J., Lindstrom, R.M., Schaef, H.T., and R.D. Orr. 2001. Distribution and Retention of ^{137}Cs in Sediments at the Hanford Site, Washington. *Environ. Science Tech*. 35:3433-3441.

Minitab 15 Statistical Software (2007). [Computer software]. State College, PA: Minitab, Inc.

Nadeau, P.H. 1999. Fundamental particles; an informal history. *Clay Minerals* 34:185-191

Paris, F., Botton, B., and F. Lapeyrie. 1995. In vitro weathering of phlogopite by ectomycorrhizal fungi. *Plant and Soil* 179:141-150.

Rovira, A.D. 1969. Plant root exudates. *The Botanical Review*. 35:35-57

Shata S, R. Hesse, R. F. Martin and H. Vali. 2003. Expandability of anchizonal illite and chlorite: Significance for crystallinity development in the transition from diagenesis to metamorphism. *Am. Mineralogist*. 748-762.

Singh, S., Negi, S., Bharati, N., and H.N. Singh. 1994. Common nitrogen control of caesium uptake, caesium toxicity and ammonium (methylammonium) uptake in the cyanobacterium (*Nostoc muscorum).* *FEMS microbiology letters*. 117:243-247.

Srodon, J., Eberl, D. D and V.A. Drits. 2000. Evolution of fundamental particle size during illitization of smectite andimplications for reaction mechanism**.** *Clays and Clay Minerals* 48:446-458

Strom, L., Owen, A.G., Godbold, D.L., and D.L. Jones. 2005. Organic acid behaviour in a calcareous soil implications for rhizosphere nutrient cycling. *Soil Bio. and Biochem.* 37:2046-2054

Sucha, V., Srodon, J., Clauer, N., Elsass,F., Eberl, D. D., Kraus, I. and J. Madejova. 2001.

Weathering of smectite and illite - smectite undertemperate climatic conditions. *Clay Minerals* 36: 403-419

Wendling, L.A., J.B. Harsh, C.D. Palmer, M.A. Hamilton, and M. Flury. 2004. Cesium sorption to illite as affected by oxalate. *Clays Clay Miner*. 52:376–382.

Wendling, L.A., J.B. Harsh, C.D. Palmer, M.A. Hamilton, and M. Flury. 2005a. Rhizosphere

effects on cesium fixation sites of soil containing micaceous clays. *Soil Sci. Am. J.* 69:1652-1657

Wendling, L.A., J.B. Harsh, C.D. Palmer, M.A. Hamilton, and M. Flury. 2005b. Cesium desorption from illite as affected by exudates from rhizosphere bacteria. *Environ. Sci. Technol.* 39:4505-4512